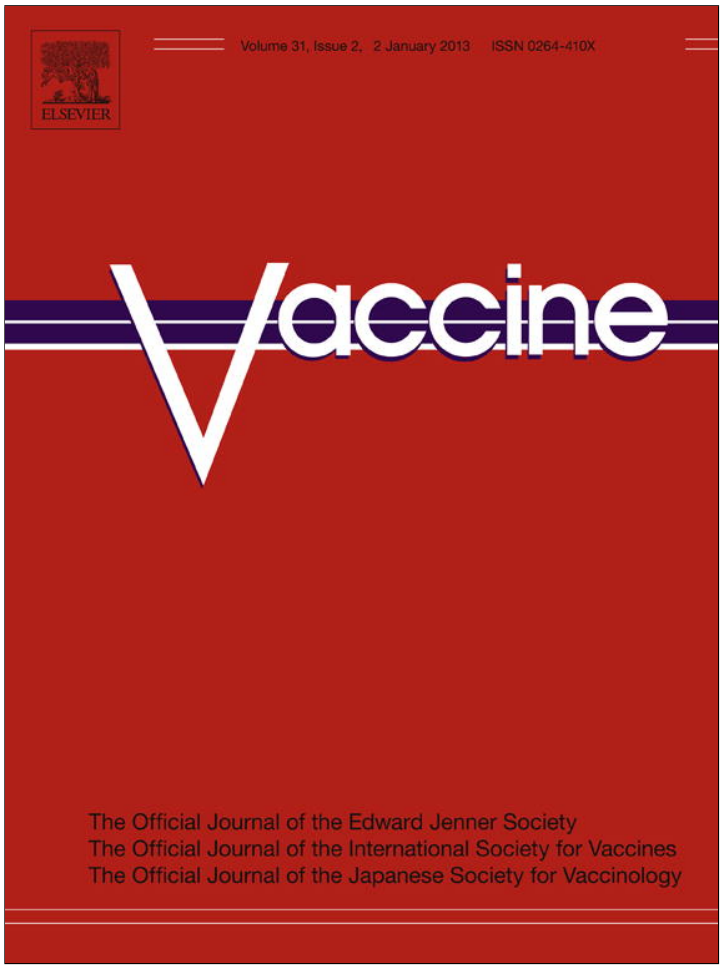

Vaccine 31 (2013) 417–424

Contents lists available at SciVerse ScienceDirect

Vaccine

journal homepage: www.elsevier.com/locate/vaccine

Chimeric hepatitis E virus-like particle as a carrier for oral-delivery

Pitchanee Jariyapong[a,b,1], Li Xing[a,1], Nienke E. van Houten[c], Tian-Cheng Li[d], Wattana Weerachatyanukul[a,b], Benjamin Hsieh[a], Carlos G. Moscoso[a], Chun-Chieh Chen[a], Masahiro Niikura[c], R. Holland Cheng[a,*]

[a] Department of Molecular and Cellular Biology, University of California, 1 Shields Ave., Davis, CA 95616, United States
[b] Department of Anatomy, Faculty of Science, Mahidol University; Bangkok 10400, Thailand
[c] Faculty of Health Sciences, Simon Fraser University, Burnaby, B.C. V5A 1S6, Canada
[d] Department of Virology II, National Institute of Infectious Diseases, Tokyo 208-0011, Japan

ARTICLE INFO

Article history:
Received 14 July 2012
Received in revised form 12 October 2012
Accepted 19 October 2012
Available online 26 October 2012

Keywords:
Hepatitis E virus
Virus like particle
Recombinant capsid protein
HIV-1 epitope
Trypsin proteolysis
Quaternary structure

ABSTRACT

Oral delivery with virus-like particles (VLPs) is advantageous because of the inherited entry pathway from their parental viral capsids, which enables VLP to withstand the harsh and enzymatic environment associated with human digestive tract. However, the repeat use of this system is challenged by the self-immunity. In order to overcome this problem, we engineered the recombinant capsid protein of hepatitis E virus by inserting p18 peptide, derived from the V3 loop of HIV-1 gp120, into the antibody-binding site. The chimeric VLP resembled the tertiary and quaternary structures of the wild type VLP and specifically reacted with an HIV-1 antibody against V3 loop. Different from the wild type VLP, the chimeric VLP was vulnerable to trypsin cleavage although it appeared as intact particle, suggesting that the intermolecular forces of attraction between the recombinant capsid proteins are strong enough to maintain the VLP icosahedral arrangement. Importantly, this VLP containing the V3 loop did not react with anti-HEV antibodies, in correspondence to the mutation at its antibody-binding site. Therefore, the insertion of peptides at the surface antigenic site could allow VLPs to escape pre-existing anti-HEV humoral immunity.

1. Introduction

Development of an effective oral delivery system for mucosal vaccination would provide a convenient means for treatment or prevention of various human diseases because it could constrain the establishment and dissemination of infection at their primary entry site, thus provide the best window of opportunity in prevention of human diseases. Despite its high efficiency, there are only a limited number of oral vaccines currently available for human utilization, far less than the number of severe health problems caused by mucosal pathogens [1]. There are several difficulties in oral immunization with non-replicating molecules, such as low pH in the stomach, the presence of proteolytic enzymes in the digestive tract, and the presence of physical as well as biochemical barriers associated with the mucosal surface itself [2]. Non-replicating virus like particles (VLPs), that inherit cell entry pathway from the viral capsid, pose a great advantage in providing desired specificity on tissue targeting and gene protection [3,4] but the major hurdle comes from their self-immunity, as shown with polyomavirus-like particle [5].

Hepatitis E virus (HEV) is a non-enveloped ssRNA virus [6] that causes human acute hepatitis through primarily fecal-and-oral transmission [7]. HEV-VLPs is a T = 1 icosahedral virus-like particles with a diameter of 270 Å [8,9]. It is self-assembled from the truncated capsid protein when it is expressed in insect cells [10] and able to induce antigen-specific mucosal immunity after oral administration [11–13]. The structure of HEV-VLP reveals a unique structural modularity, i.e. the three domains of the truncated protein carry independently the biological functions [14–16]. While the N-terminal S domain (shell; amino acids 118–317) forms icosahedral base [14–16] and the adjacent M domain (middle; amino acids 318–451) builds up the three-fold plateau, the P (protruding; amino acids 452–606) domains exhibits profound HEV antigenicity [14,17,18], dimerization [19,20], and host recognition [21]. As a result, sequence modification at the P-domain will not interfere with HEV-VLP assembly as well as the stability of the VLP in acidic and proteolytic environment. In fact, a chimeric VLP carrying a peptide insertion at C-terminal end of the truncated capsid protein retains the T = 1 icosahedral organization [12]. If an insertion can be placed at antibody-binding site at the P-domain, the chimeric VLP may be able to escape from antibody-binding. However, it requires insertion of foreign epitope in the middle region of PORF2, and four

* Corresponding author. Tel.: +1 530 752 5659.
E-mail address: rhch@ucdavis.edu (R.H. Cheng).
[1] These authors have contributed equally to this work.

0264-410X/$ – see front matter © 2012 Elsevier Ltd. All rights reserved.
http://dx.doi.org/10.1016/j.vaccine.2012.10.073

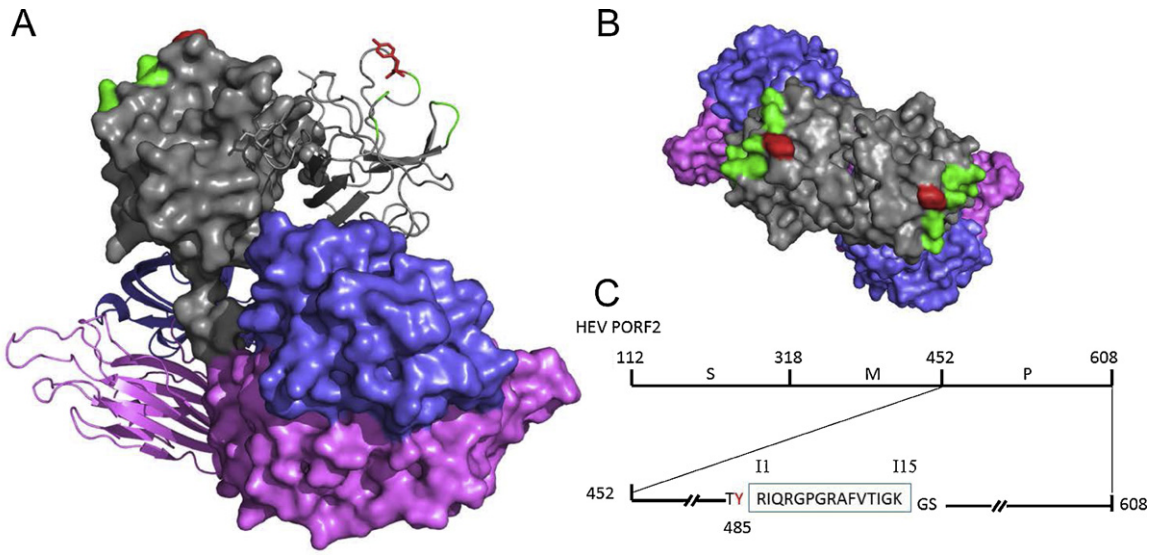

Fig. 1. Schematic diagram of the chimeric p18-VLPs. (A) side view of a PORF2 dimer colored in magenta for the S-domain, slate for the M-domain and gray for the P-domain. The residue Y485 (red stick) is overlapped with the binding site of HEP224 antibody (green colored surface). (B) Top view of the dimer showing the spatial arrangement of Y485 (red) and the binding site of HEP224 antibody (green). (C) Insertion of 15 amino acid residues of p18 (boxed; I1-I15) at the position 485 (red) of P-domain indicated by arrowhead (bottom). (For interpretation of the references to color in this figure legend, the reader is referred to the web version of the article.)

previous trials at residues A179, R366, A507 and R542 had all failed [12] because the insertions were found to inhibit the quaternary assembly of the VLP [22]. With the known crystal structure and a well-defined antibody-binding site, we selected an insertion site after residue Tyr485. Our results indicate that the chimeric VLP carrying the insertion at Tyr485 is stable within hydrolytic and proteolytic environments, and is thus suitable for oral delivery.

2. Results

2.1. Reaction of p18-VLP to antibodies

The P-domain of HEV organizes into a β-barrel consisting of two β-sheets, the F″A″Bb″ sheet and the Ba″E″D″C″ sheet. The residue Y485 is located at the A″Ba″ loop and is within the binding interface of HEP224, a conformational anti-ORF2 antibody. The A″Ba″ loop is positioned at the shoulder of the protruding P-domain and hangs down to cover a surface groove region. This leads to a slightly higher B-factor for the residues around Y485 and the groove provides sufficient space to accommodate additional amino acids (Fig. 1A and B). Thus the residue Y485 was identified as a promising candidate for insertion of a short peptide without interfering with either tertiary structure folding or capsid assembly.

To test our hypothesis, we constructed a fusion protein by inserting a 15-amino acid antigenic peptide, “p18”, after residue Y485 on the P-domain of HEV-VLPs (Fig. 1C). The p18 epitope (RIQRGPGRAFVTIGK) is from the V3 loop of the HIV-1 Env subunit gp120, which is able to stimulate an HIV-1-specific cytotoxic T-lymphocyte (CTL) response [23]. The fusion protein was recovered after CsCl density gradient purification in a form of chimeric virus-like particles (Fig. 2A), referred as “p18-VLPs”. We then assessed the reactivity of p18-VLP to two antibodies 447-52D and HEP224 specific against the V3 loop of HIV-1 Env gp120 and a conformational epitope of the wild type HEV, respectively. As a reference, the reactivity of 0.1 mg/ml wild-type HEV-VLP to antibody HEP224 was set as 100% (Fig. 2B). The antibody 447-52D was found to react preferably with the p18-VLPs (50% to 0.001 mg/ml and 100% to 0.1 mg/ml p18-VLP). Although nonspecific binding was observed in wild-type HEV-VLP at all concentrations, the level was constantly less than 30% reactivity. Strikingly, the reactivity of HEP224 to p18-VLPs was very low. Only 1–2% HEP224 reactivity to 0.1 mg/ml p18-VLP was detected, in contrast to the 100% reactivity to 0.1 mg/ml wild-type HEV-VLP, although 0.1 mg/ml p18-VLP showed 100% reactivity to the antibody 447-52D. These results indicated a successful insertion of p18 peptide after residue Y485, which in turn disrupted the binding interface to antibody HEP224 but enabled the binding to 447-52D antibody.

2.2. The assembly of p18-VLP

The p18-VLP appeared as a spherical projection decorated with spikes on a surface profile (Fig. 2A). The projection image showed light density in the center, suggesting that the VLP was free of nucleic acid, like the wild-type HEV-VLP. The cryo-EM map revealed 30 protruding spikes positioned at each of the icosahedral two-fold axes (Fig. 3). Close investigation of the density radial distribution revealed several minor differences between p18- and HEV-VLPs. The density of the P domain appeared thicker in p18-VLP at a radius of 120 Å and two subunits appeared weakly associated than that in the wild-type VLP (Fig. 3). The density of p18-VLP at radius of 110 Å rotated slightly clockwise from that in the the wild type VLP, although the M-domain remained at the same orientation (r = 102 Å) in both VLPs. Thus, the insertion of p18 peptide did not interfere with VLP icosahedral base; instead it modified slightly the orientation of the P-domain. The coordinates of PORF2 subunits agreed well with the cryo-EM density map of p18-VLP (Fig. 4 A). No adjustment was needed to fine-tune the lateral contacts between subunits. The coordinates of three domains were in good consistence to the density of icosahedral shell, the threefold plateau, and the protruding spikes, except the flexible hinge loop between the M- and P-domains (Fig. 4B). Therefore, the chimeric PORF2 retained the tertiary and quaternary structure of HEV wild type VLP. Most notably, the P-domain demonstrated the same intermolecular contacts as the wild type, despite of local proteolytic cleavage in individual subunits.

2.3. Susceptibility to proteolytic digestion

The sequence of p18 peptide is rich in positively-charged amino acids and contains three arginines at positions I1, I4, and I8 as well as one lysine at position I15 (Fig. 1). Insertion of such a sequence in

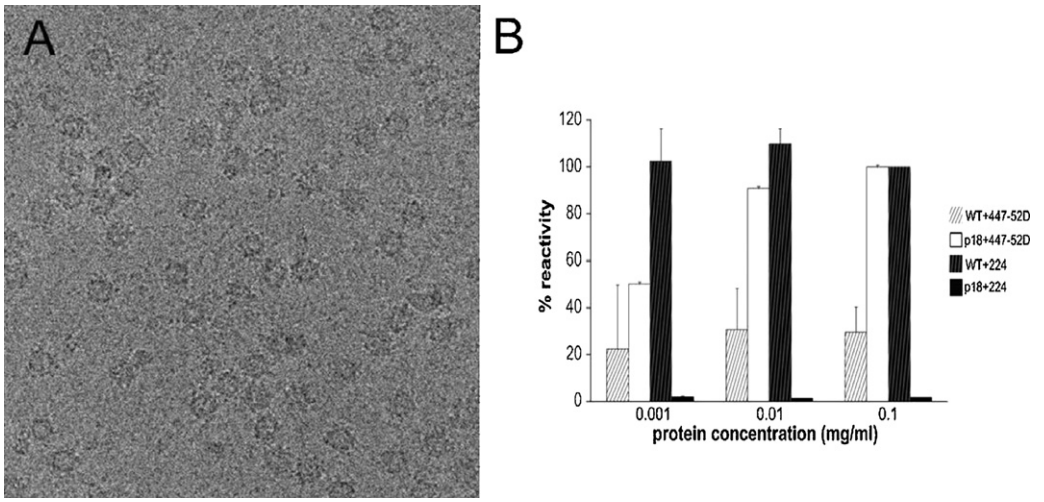

Fig. 2. The characterization of p18-VLPs. (A) Cryo-electron micrograph of frozen-hydrated p18-VLP. (B) Reactivity of antibodies HIV447-52D (white bars) and HEV224 (black bars) to the p18-VLPs (non-striated) and WT-VLPs (striated) as determined by ELISA. The data are averaged from triplicate experiments and are expressed as mean ± S.D. Note high immunoreactivity of p18-VLPs with anti-HIV447-52D but it is completely diminished with anti-HEV224.

the middle of a solvent-exposed region of a viral capsid may introduce vulnerable sites for trypsin cleavage, a feature that did not exist in the original protein. As tested by immunoblotting using anti-HIV-1 antibody 447-52D, a single immune-reactive band was detected at a position corresponding to a molecular weight of 53 kD from the samples purified in the presence of protease inhibitor (Fig. 5A). Without the protease inhibitor, a weakly immunoreactive band of 42 kD in molecular weight was observed from the sample collected at 6 days p.i., in addition to the 53 kDa band (Fig. 5A). Upon storage of 25 days in the absence of protease inhibitor, the intensity of the 42 kD peptide increased dramatically (Fig. 5A) in corresponding to the decrease of the 53 kD peptide. However, the intensity of the immune-reactive band at 42 kD remained undetectable if protease inhibitor was added (Fig. 5A). These results indicated possible protease cleavage and the cleavage may occur at the insertion region, most likely at the C-terminal end of p18 (I15) because the

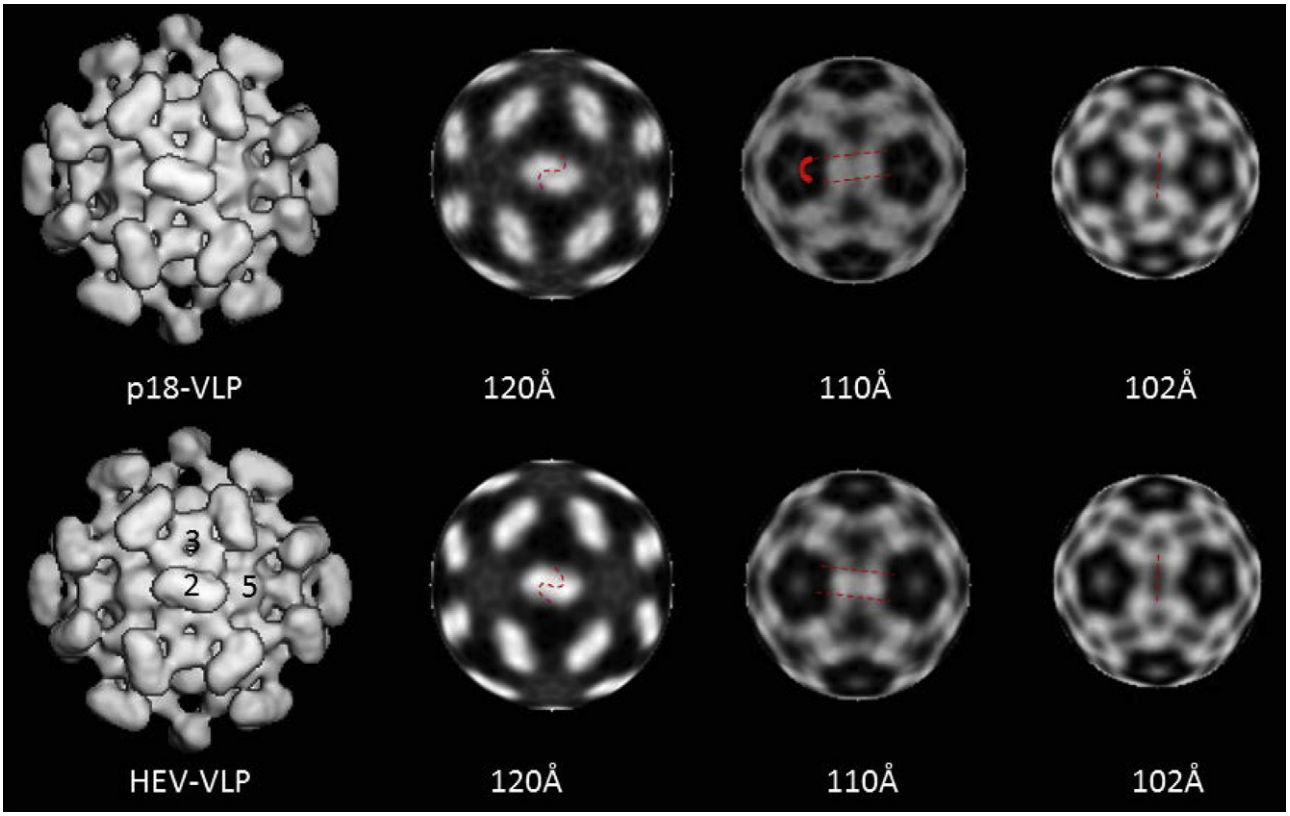

Fig. 3. Three-dimensional density maps of p18-VLP (top panel) and the wild type HEV-VLPs (bottom panel). The surface rendering map shows that the p18-VLP resembles the appearance of HEV-VLP and contains spike and plateau at 2fold- and 3-fold axes, respectively (the position of icosahedral axes is labeled with the corresponding number). The particles were sliced into thin sections to show the density distribution at radii of 120 Å (the P-domain), 110 Å (the M-domain) and the 102 Å (the S-domain). The red dashed lines profile the difference between the p18-VLP and the wild type HEV-VLP.

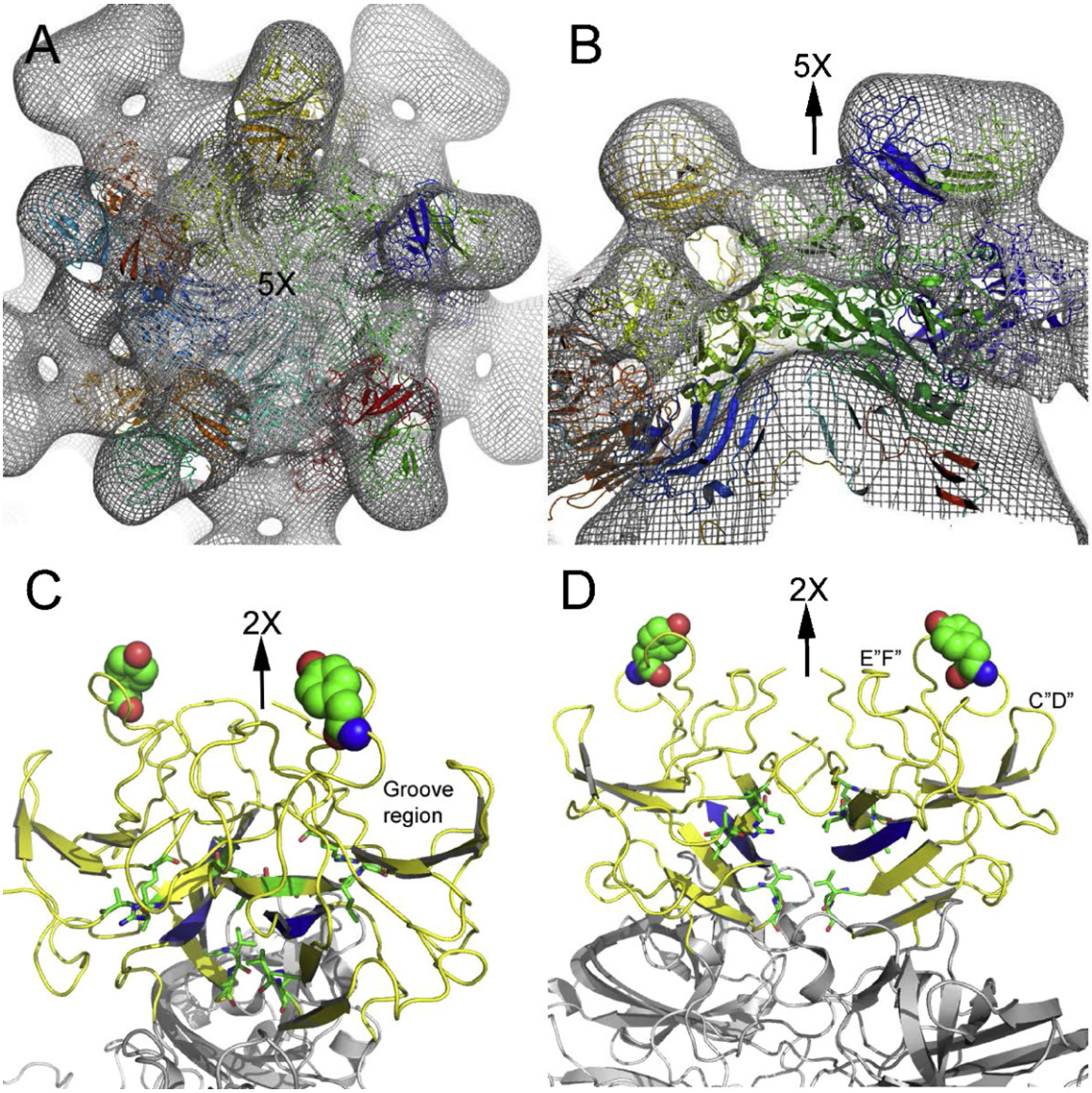

Fig. 4. Fitting of p18-VLP cryo-EM density map with the crystal structure of the HEV-VLP. The coordinates of PORF2 decamer (pentamer of dimers) agreed well with the cryo-EM density map at 5fold-axis region (A) and with the separation of S-, M- and P-domain (B). Ribbon presentation of a PORF2 dimer showing the position of surface groove region (C) and the hydrophobic residues (stick presentations) at the P-domain dimeric interface (D).

calculated mass of the fragment from residue 112–485 (40.5 kDa) agreed well with the measured one and the p18 immunogenicity is integrated with the 42 kDa fragment.

2.4. Resistance to trypsin and pepsin treatment

In order to test the stability of the chimeric VLPs in a highly proteolytic milieu, we further investigated the proteolytic digestion of the purified p18-VLPs with trypsin and pepsin, two enzymes that are present abundantly in the digestive tract. Because the 42 kD peptide remains immunoreactive with anti-HIV-1 antibody 447-52D, i.e. the enzyme cleavage site is most likely at the C-terminal end of the p18 insertion; therefore, trypsin is the dominant enzyme in this reaction. In the presence of trypsin, the 53 kDa band disappeared while the 42 kDa band remained unchanged (Fig. 5B). There was no extra band observed after silver staining. In contrast, the wild-type VLPs remained resistant to trypsin treatment (data not shown). Like trypsin, pepsin is an enzyme in stomach that cleaves peptide bonds between hydrophobic and preferably aromatic amino acids and did not enhance trypsin digestion of intact p18-VLP. After disassembly by the mixture of EDTA and DTT, the combination of trypsin and pepsin enhanced proteolytic digestion of PORF2 individual dimers. It further digested 42 kD peptide into short peptides of multiple lengths that appeared as extra bands in SDS-PAGE. We then investigated whether protease cleavage of p18-VLP disassembles the VLP structure. We then investigated whether protease cleavage disrupted the structure of p18-VLP. We treated p18-VLP with 30 mU/ml of trypsin for one hour and examined the treated p18-VLP via electron microscopy. The negatively stained p18-VLPs appeared as empty ring-like profiles covered with spikes (Fig. 5C). The measured diameter of the projection was ~25 nm, consistent with the diameter reported for the T = 1 HEV-VLP. Therefore, this data demonstrated that the p18-VLP maintained the VLP structure after proteolytic cleavage and retained the resistance to hydrolytic enzyme.

The structural integrity of p18-VLP is further demonstrated by the consistency between the structures of VLPs with and without p18 insertion (Fig. 4A and B). Therefore, the chimeric PORF2 retained the tertiary structure of properly folded PORF2, and assembled into a quaternary structure resembling the VLP of wild type in

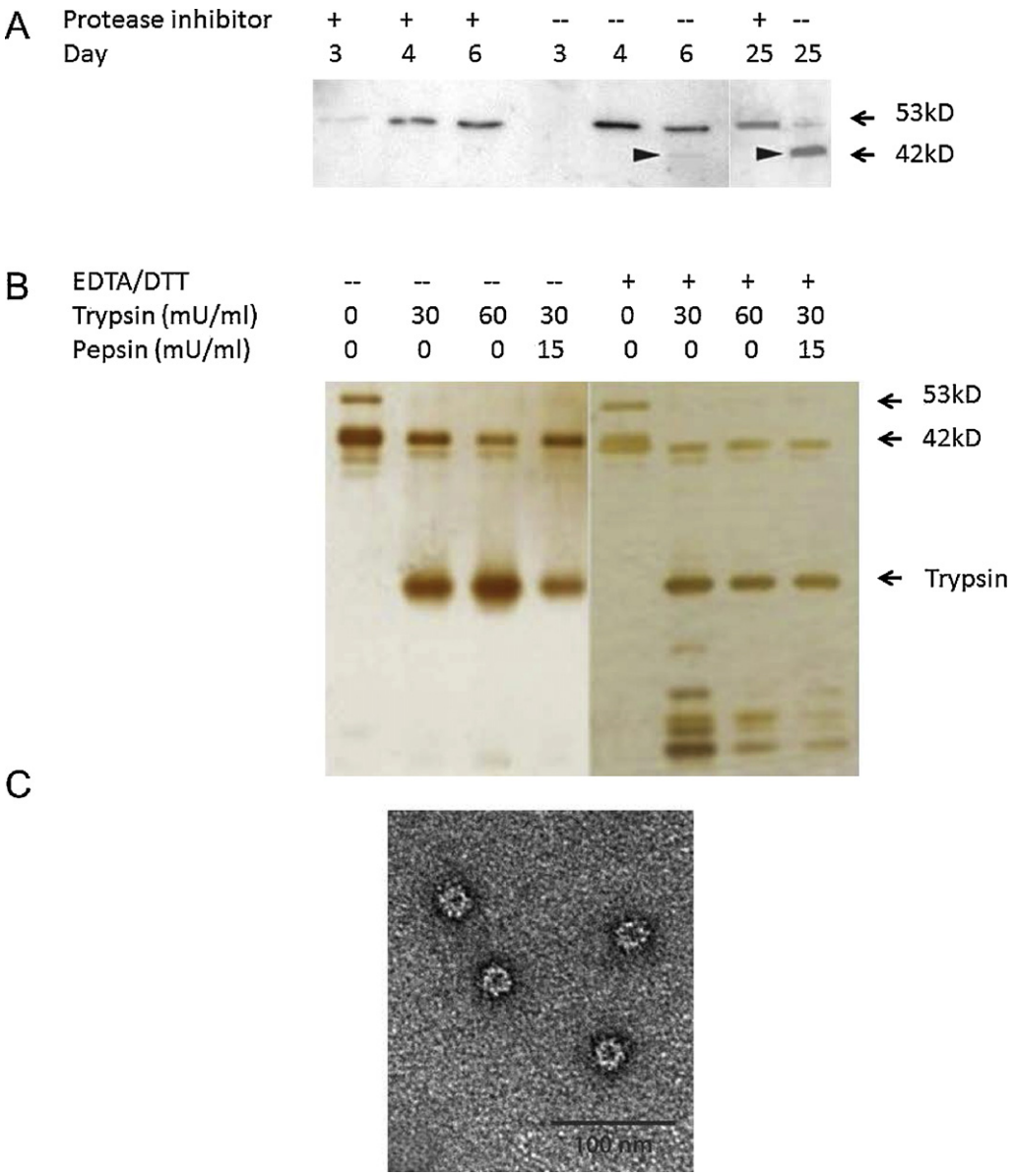

Fig. 5. Hydrolysis of the p18-VLPs. (A) VLPs recovered from the culture media in the presence (+)/absence (−) of protease inhibitors were subjected on SDS-PAGE under reducing condition and then immunoblotted with anti-HIV-1 antibody 447-52D. (B) Electrophoresis result of the p18-VLP pretreated with EDTA/DTT, 30 mU/ml or 60 mU/ml trypsin, and 15 mU/ml pepsin. The SDS-PAGE was performed under reducing condition and developed with silver staining. (C) Electron micrograph of negatively stained p18-VLPs after treatment with 60 mU trypsin. Bars = 100 nm.

the organization of domain display and the subunit contact. Most notably, the protruding spike of the p18-VLP remained in association as dimeric units on top of the intact icosahedral shell, despite of local proteolytic cleavage in individual subunits.

3. Discussion

Virus-like particles have gained increasing interest in vaccine development due to multiple reasons. The effect of their delivery depends largely on the insertion site where the foreign epitope can be well-integrated into VLP structure without causing interference with VLP assembly. The exposed terminus of the capsid protein is the common choice for such task. However, with a known crystal structure, a peptide insertion can be arranged at surface antigenic loop without disturbing the VLP structure to reduce the reactivity to the given antibodies.

The antigenic domain of HEV is reported as conformational and a handful of amino acids were determined as essential to antibody binding by mutagenesis [16,24]. They can be grouped as two surface patches located at the two opposite sides of the P-domain (Fig. 6A). The binding site of antibody HEP224 is composed of three surface loops around residue Tyr485 [22]. Insertion of p18 peptide at Tyr485 disrupted the interaction of these loops leading to conformational rearrangement. As a result, the newly defined the loop organization is no long complimentary to HEP224 paratope and inhibits the binding of other antibodies that recognize the same location as HEP224 (data not shown). Insertion of p18 peptide does not shield completely the antigenic domain; therefore further mutation is necessary to fully block the response of HEV-VLP to the pre-existing anti-HEV antibodies.

Trypsin cleavage did not eliminate the antigenicity of p18 when inserted after residue Y485, since the 42 kD peptide is immunoreactive to antibody 447-52D. This chimeric VLP can thus be used as vector to deliver protein antigen and more immunological experiment is necessary. However, the p18-peptide, when exposed on the surface of VLP by insertion at C-terminal end of PORF2, is

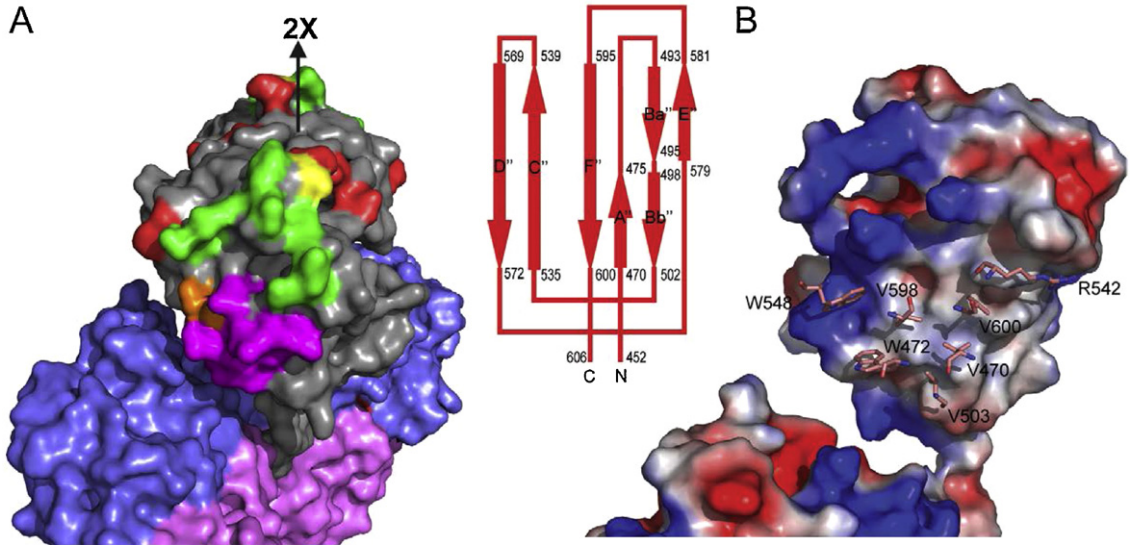

Fig. 6. Antigenic structure and dimeric interface of the P-domain. (A) Surface presentation of a HEV dimer, in which the P-, M-, and S-domain are colored in gray, slate blue, and light pink, respectively. The antibody-binding amino acids identified by mutagenesis are colored in the red. They overlap with HEP224 binding-site (green) at residue S487 (yellow) and with 8C11 binding-site (magenta) at residue D496 (colored in brown). (B) Surface potential representation of PORF2 mononer to show the dimeric contacting interface at the P-domain. The blue region is positively charged while the red region is negatively charge and the white region is non-polar. The amino acids of the ball-and-stick model are labelled to show residues that are critical for dimer formation. (For interpretation of the references to color in this figure legend, the reader is referred to the web version of the article.)

able to induce HIV-1 V3 loops specific antibody in mice (data not shown). Nevertheless, peptide remains surface-exposed to be recognized by the target molecules when inserted after residue Y485 of PORF2.

The three-dimensional reconstruction of the p18-VLP showed little difference to the structure of wild-type VLPs, even when subjected to an enzymatic environment. Trypsin cleavage most likely occurred at the C-terminal end (I15) of the inserted p18 peptide and did not induce spike disassociation from the icosahedral shell. This can be explained by the intermolecular forces of attraction that hold the quaternary structure of HEV-VLP (Fig. 6B). The hydrophobic effect is the primary weak force stabilizing the folding of the P-domain as well as its interaction between two P-domains within the same spike. There are 28 hydrophobic amino acids lining within the P-domains and five of them are from the β-strand A″ (amino acids 470-475) which is well protected by the β-sheet F″A″Bb″. The strong hydrophobic interactions hold the association of β-strand A″ to the C-terminal fragment after trypsin cleavage at residue I15 and tighten up the connection of the C-terminal fragment to icosahedral shell. Thus, the hydrophobic core of the P-domain actually protects p18-VLP integrity so that the VLP remained intact even in a proteolytic environment.

In conclusion, we reported a chimeric HEV-VLP that carried a foreign epitope at outermost surface that induces conformational changes at antigenic domain while maintains the tertiary and quaternary structures as well as the biological resistance to proteolytic enzymes. Moreover, the antigenic peptide can be replaced with a short peptide sequence. It has be reported that attachment to M cells at guts epithelium initiates antigen-specific mucosal immune responses [25] and that the α5β1 integrin is uniquely distributed on the apical surface of M cells but on the lateral and basolateral surfaces of neighboring enterocytes [26]. It is therefore possible to design a chimeric HEV-VLP carrying an Arg-Gly-Asp (RGD) integrin-binding motif to enhance M-cell uptake [27], and even carrying a targeting molecules to retarget HEV-VLP to particular cell types, e.g. RGD motif to retarget angiogenic endothelial cells by interacting with the overexpressed integrin receptors [28]. Angiogenesis, a process for the formation of new capillary blood vessels, has a crucial role in solid tumor progression and the development of metastasis. RGD-functionalized HEV-VLP therefore provides a safe and non-invasive vector for cancer antiangiogenic therapy, which is designed to arrest the growth or spread of tumors.

4. Materials and methods

4.1. Cloning of p18 sequence into position 485 of PORF2-HEV

To insert the HIV-1 p18 epitope into the PORF2 gene, the baculovirus transfer vector carrying the PORF2 gene (pFastBac1/PORF2-HEV/MluI) was mutated to create a unique *Mlu*I at the desired location. The QuikChange® Site-directed Mutagenesis Kit (Stratagene, La Jolla, CA) was used according to the manufacturer's instructions to change base pairs at position 1457 (G to C) and 1458 (C to G) so as to create an *Mlu*I restriction enzyme site that corresponds to position 485 in the protein sequence in PORF2-HEV. The mutagenesis primers HEVMluFwd (5′GACCAGTCCACTTACG**CG**TCTTCGACCGGCCCA3′) and HEVMluRev (5′TGGGCCGGTCGAAGACGCGTAAGTGGACTGGTC3′) were used for this purpose. This resulted in a relatively conservative Gly to Ala change at position 486 in PORF2. Positive clones were confirmed by screening plasmids for the presence of the newly created *Mlu*I restriction enzyme site (pFastBac1/PORF2-HEV/MluI) by *Mlu*I digestion.

Two overlapping phosphorylated oligonucleotides, p18pos#485Top (5′phos CGCGTCGCGTATCCAGAGGGGACCAGGGAGAGCATTTGTTACAATAGGAAAAGA) and p18pos#485Bottom (5′phos CGCGTCTTTTCCTATTGTAACAAATGCTCTCCCTGGTCCCCTCTGGATACGCGA 3′), encoding the p18 epitope sequence flanked by *Mlu*I ends, were annealed and ligated to *Mlu*I-digested pFastBac1/PORF2-HEV/MluI. Clones were screened for correct insertion and orientation by DNA sequencing (pFastBac1/PORF2-HEV/P18pos#485).

4.2. Production and purification of p18-VLP

The recombinant baculovirus vectors used to express VLPs bearing p18 epitopes were generated using the Bac-to-Bac® Baculovirus Expression System [8–10]. The p18-VLPs were collected and purified through multiple steps of ultracentrifugation and CsCl equilibrium density gradient. The purified p18-VLP was stored in 10 mM potassium-MES buffer (pH 6.0) in the presence/absence of protease inhibitors (1:50, v/v).

4.3. Enzymatic digestions of p18 HEV-VLPs and protein characterization

Proteolytic treatment was carried out for one hour at room temperature. Disassembly of p18-VLPs were done in a buffer containing 50 mM Tris–HCl (pH 7.5) 1 mM ethylene glycol tetra-acetic acid (EGTA), 20 mM dithiothreitol (DTT), and 150 mM NaCl for 1 h at room temperature. The products of cleavage were then analyzed by SDS-PAGE under reducing conditions and stained using a commercial silver staining kit from Invitrogen.

4.4. ELISA to detect binding to HEP 224 and 447-52D

The 96-well plate was coated with VLP and interacted with anti-HEV antibody HEP 224 and anti-HIV-1 antibody 447-52D. The antibody reaction was detected by alkaline phosphatase-labeled secondary antibodies and developed using p-nitrophenylphosphate solution.

4.5. Negative staining of proteolyzed p18-VLPs

The reaction mixtures were loaded onto a glow-discharged, carbon-coated EM grids and stained with 2% uranyl acetate. The samples were examined under a JEOL-1230 transmission electron microscope (TEM) and the images were recorded on a CCD camera (TVIPS Gauting, Germany) at a magnification of 40,000×.

4.6. Cryo-EM and three-dimensional image reconstruction

Cryo-EM and sample preparation were performed according to the previously described protocol [9]. The specimen was transferred into a JEOL 2100F TEM with a Gatan 626 cryo transfer system and the micrographs were recorded under a low-dose condition (<10 electrons/Å^2) on a TVIPS CCD camera at an interval of 2 Å at specimen space. Micrographs exhibiting minimal astigmatism and specimen drift were selected for image processing. The origin and orientation of each individual particle was first estimated and refined using a model-based polar Fourier transform (PFT) method [29,30]. The three-dimensional density map was computed with superimposing 5-3-2 icosahedral symmetry. The final density map was reconstructed from 945 individual particles with the final resolution at 15.3 Å assessed with Fourier shell correlation by taking correlation coefficient of 0.5 as cutoff. The fitting was carried out initially with program O [31] and refined Situs autofitting program [31–34] and was stopped when the cross correlation coefficient reached 80%. The final figures were generated using PyMOL [35].

Acknowledgment

The authors thank Dr. Tatsuo Miyamura for the supportive guidance. This study was funded by grants of NIH NCI pilot, NIH grant (AI095382) and UC Discovery Programs. PJ and WW were supported in part by a research grant from the Commission on Higher Education (CHE), and Faculty of Science at Mahidol University in Thailand.

References

[1] Holmgren J, Czerkinsky C. Mucosal immunity and vaccines. Nat Med 2005;11:S45–53.
[2] Ogra PL, Faden H, Welliver RC. Vaccination strategies for mucosal immune responses. Clin Microbiol Rev 2001;14:430–45.
[3] Ludwig C, Wagner R. Virus-like particles-universal molecular toolboxes. Curr Opin Biotechnol 2007;18:537–45.
[4] Uchida M, Klem MT, Allen M, Suci P, Flenniken M, Gillitzer E, et al. Biological containers: protein cages as multifunctional nanoplatforms. Adv Mater 2007;19:1025–42.
[5] Clark B, Caparros-Wanderley W, Musselwhite G, Kotecha M, Griffin BE. Immunity against both polyomavirus VP1 and a transgene product induced following intranasal delivery of VP1 pseudocapsid-DNA complexes. J Gen Virol 2001;82:2791–7.
[6] Tam AW, Smith MM, Guerra ME, Huang CC, Bradley DW, Fry KE, et al. Hepatitis E virus (HEV): molecular cloning and sequencing of the full-length viral genome. Virology 1991 Nov;185(1):120–31.
[7] Emerson S, Purcell R. Hepatitis E virus. In: Knipe DM, Howley PM, editors. Fields Virology. Fifth ed. Philadelphia: Lippincott Willimas & Wilkins; 2007. p. 3047–58.
[8] Li T-C, Takeda N, Miyamura T, Matsuura Y, Wang JCY, Engvall H, et al. Essential elements of the capsid protein for self-assembly into empty virus-like particles of hepatitis E virus. J Virol 2005;79(October (20)):12999–3006.
[9] Xing L, Kato K, Li T, Takeda N, Miyamura T, Hammar L, et al. Recombinant hepatitis E capsid protein self-assembles into a dual-domain T = 1 particle presenting native virus epitopes. Virology 1999;265(December (1)):35–45.
[10] Li TC, Yamakawa Y, Suzuki K, Tatsumi M, Razak MA, Uchida T, et al. Expression and self-assembly of empty virus-like particles of hepatitis E virus. J Virol 1997;71(October (10)):7207–13.
[11] Takamura S, Niikura M, Li TC, Takeda N, Kusagawa S, Takebe Y, et al. DNA vaccine-encapsulated virus-like particles derived from an orally transmissible virus stimulate mucosal and systemic immune responses by oral administration. Gene Ther 2004;11(April (7)):628–35.
[12] Niikura M, Takamura S, Kim G, Kawai S, Saijo M, Morikawa S, et al. Chimeric recombinant hepatitis E virus-like particles as an oral vaccine vehicle presenting foreign epitopes. Virology 2002;293(February (2)):273–80.
[13] Li T, Takeda N, Miyamura T. Oral administration of hepatitis E virus-like particles induces a systemic and mucosal immune response in mice. Vaccine 2001;19(May (25–26)):3476–84.
[14] Xing L, Li TC, Miyazaki N, Simon MN, Wall JS, Moore M, et al. Structure of hepatitis E virion-sized particle reveals an RNA-dependent viral assembly pathway. J Biol Chem 2010;285:33175–83.
[15] Guu T, Liu Z, Ye Q, Mata D, Li K, Yin C, et al. Structure of the hepatitis E virus-like particle suggests mechanisms for virus assembly and receptor binding. Proc Natl Acad Sci U S A 2009;106:12992–7.
[16] Yamashita T, Mori Y, Miyazaki N, Cheng H, Yoshimura M, Unno H, et al. Biological and immunological characterics of hepatitis E virus-like particles based on the crystal structure. Proc Natl Acad Sci U S A 2009;106:12986–91.
[17] Schofield DJ, Purcell RH, Nguyen HT, Emerson SU. Monoclonal antibodies that neutralize HEV recognize an antigenic site at the carboxyterminus of an ORF2 protein vaccine. Vaccine 2003;22(December (2)):257–67.
[18] Zhang J, Gu Y, Ge SX, Li S, He Z, Huang G, et al. Analysis of hepatitis E neutralization sites using monoclonal antibodies directed against a virus capsid protein. Vaccine 2005;23:2881–92.
[19] Li X, Zafrullah M, Ahmad F, Jameel S. A C-terminal hydrophobic region is required for homo-oligomerization of the hepatitis E virus capsid (ORF2) protein. J Biomed Biotechnol 2001;1(3):122–8.
[20] Li S, Tang S, Seetharaman J, Yang CY, Gu Y, Zhang J, et al. Dimerization of hepatitis E virus capsid protein E2s domain is essential for virus-host interaction. PLos Pathog 2009;5(8):e1000537.
[21] Yu H, Li S, Yang CY, Wei M, Song C, Zheng Z, et al. Homology model and potential virus-capsid binding site of a putative HEV receptor Grp78. J Mol Model 2010 [Epub ahead of print].
[22] Xing L, Wang JC, Li TC, Yasutomi Y, Lara J, Khudyakov Y, et al. Spatial configuration of hepatitis E virus antigenic domain. J Virol 2011;85(January (2)):1117–24.
[23] Takahashi H, Cohen J, Hosmalin A, Cease KB, Houghten R, Cornette JL, et al. An immunodominant epitope of the human immunodeficiency virus envelope glycoprotein gp160 recognized by class I major histocompatibility complex molecule-restricted murine ctyotoxic T lymphocytes. Proc Natl Acad Sci U S A 1988;85:3105–9.
[24] Zhou YH, Purcell R, Emerson S. A truncated ORF2 protein contains the most immunogenic site on ORF2: antibody responses to non-vaccine sequences following challenge of vaccinated and non-vaccinated macaques with hepatitis E virus. Vaccine 2005;23:3157–65.
[25] Kyd JM, Cripps A. Functional differences between M cells and enterocytes in sampling luminal antigens. Vaccine 2008;26:6221–4.
[26] Gullberg E, Keita AV, Salim SY, Andersson M, Caldwell KD, Söderholm JD, et al. Identification of cell adhesion molecules in the human follicle-associated epithelium that improves nanoparticle uptake into the Peyer's patches. J Pharmacol Exp Ther 2006;319(2):632–9.
[27] Clark M, Hirst BH, Jepson M. M-cell surface b1 integrin expression and invasin-mediated targetting of *Yersinia pseudotuberculosis* to mouse Peyer's patch M cells. Infect Immun 1998;66:1237–43.

[28] Ruoslahti E. RGD and other recognition sequences for integrins. Annu Rev Cell Dev Biol 1996;12:697–715.
[29] Baker TS, Cheng RH. A model-based approach for determining orientations of biological macromolecules imaged by cryoelectron microscopy. J Struct Biol 1996;116(January–February (1)):120–30.
[30] Baker TS, Cheng RH. A model-based approach for determining orientations of biological macromolecules imaged by cryoelectron microscopy. J Struct Biol 1996;116(1):120–30.
[31] Jones TA, Zou JY, Cowan SW, Kjeldgaard M. Improved method for building protein model in electron density maps and the location of errors in these models. Acta Crystallogr Sect A 1991;47:110–9.
[32] Wriggers W. Using situs for the integration of multi-resolution structures. Biophys Rev 2010;2:21–7.
[33] Xing L, Li TC, Mayazaki N, Simon MN, Wall JS, Moore M, et al. Structure of hepatitis E virion-sized particle reveals an RNA-dependent viral assembly pathway. J Biol Chem 2010;285(43):33175–83.
[34] Xing L, Wang JC, Li T-C, Yasutomi Y, Lara J, Khudyakov Y, et al. Spatial configuration of hepatitis E virus antigenic domain. J Virol 2011;85: 1117–24.
[35] DeLano WL. The PYMOL molecular graphics system. Palo Alto, CA, USA: DeLano Scientific; 2002.